GEOPHYSICAL RESEARCH LETTERS, VOL. 33, L24609, doi:10.1029/2006GL027399, 2006

Structure and origin of the subtropical South Indian Ocean Countercurrent

Gerold Siedler,[1] Mathieu Rouault,[2] and Johann R. E. Lutjeharms[2]

Received 29 June 2006; revised 29 September 2006; accepted 14 November 2006; published 21 December 2006.

[1] The structure of the subtropical South Indian Ocean Countercurrent (SICC) is revealed by altimeter-derived absolute geostrophic surface velocities. It is a narrow, eastward-flowing current between 22° and 26°S confined to planetary wave trains which propagate westward through the Indian Ocean. Multi-year averaging identifies it as a well-defined current between Madagascar and 80°E, continuing with lower intensity between 90° and 100°E. It virtually coincides with the northern limit of Subtropical Underwater subduction. Geostrophic currents from hydrographic sections closely correspond to these surface patterns. Volume transports of the countercurrent down to 800 dbar are of order (10^7 m^3 s^{-1}). Evidence is provided for a narrow branch of the South Equatorial Current (SEC) approaching Madagascar near 18°S and feeding the southern East Madagascar Current (EMC) which appears to continue westward around the southern tip of Madagascar. It then partially retroflects and nourishes the SICC. **Citation:** Siedler, G., M. Rouault, and J. R. E. Lutjeharms (2006), Structure and origin of the subtropical South Indian Ocean Countercurrent, *Geophys. Res. Lett.*, *33*, L24609, doi:10.1029/2006GL027399.

1. Introduction

[2] Broad zonal bands of high current variability in the western regions of subtropical gyres have been related to eastward currents in the North Atlantic [e.g., *Rossby et al.*, 1983], the North Pacific [*Wyrtki*, 1975; *Aoki and Imawaki*, 1996; *Qiu*, 1999] and in the South Pacific Ocean [*Merle et al.*, 1969; *Qiu and Chen*, 2004]. Wide eastward surface geostrophic flows in the South Indian Ocean were also displayed in the mean surface topographies by *Wyrtki* [1971], *Reid* [2003], *Rio and Hernandez* [2004], and *O'Connor et al.* [2005]. However, the eastward geostrophic flow in the South Indian Ocean was only recently perceived as a distinct and shallow countercurrent [*Palastanga et al.*, 2006]. New data sets based on the mean topography of *Rio and Hernandez* [2004] and sea level anomalies now permit study of the detailed structure of the countercurrent both in space and time, and a search for the possible origin of the flow. Combining the results with hydrographic sections provides new knowledge on its deeper vertical structure and typical transports. We will use the name South Indian Ocean Countercurrent (SICC) henceforth which was suggested by *Palastanga et al.* [2006].

2. Method and Data

[3] The new method of combining altimetry, in situ observations and an improved geoid model by *Rio and Hernandez* [2004] provides an improved mean absolute dynamic topography of the global ocean. They applied an iterative process by first subtracting an available geoid from satellite mean sea surface height (SSH), then merging with the World Ocean Data Base 1998 climatology [*Levitus et al.*, 2001] to provide shorter spatial scales, and finally combining in situ measurements with altimetric data. The in situ data include drifter velocities [*Niiler et al.*, 1995; *Hansen and Poulain*, 1996] and XBT and CTD casts from a 1993–2000 data set which possibly includes some of the data already used by Levitus. Error estimates for mean geostrophic velocities resulting from this method are below 10 cm/s at middle and low latitudes. The data are therefore suitable for studying strong currents in subtropical regions.

[4] The data set developed here to characterize the mid-latitude South Indian Ocean is based on absolute geostrophic currents resulting from the sum of the mean dynamic topography (scale 660 km) and sea level anomaly (scale 1/3° or about 35 km) from August 2001 to May 2006 (www.aviso.oceanobs.com). The resolution both in space and in time is higher than in any large-scale in situ observational data set.

3. Planetary Waves, Eddies, and the Countercurrent

[5] As reviewed by *Stramma and Lutjeharms* [1997], the overall upper-layer circulation in the region of study is dominated by the counterclockwise South Indian subtropical gyre. Transport patterns include anticyclonic flow centered in the western Indian Ocean, with mostly westward transports at mid-latitudes between about 15°S and 35°S. It is also well known that long westward-propagating planetary waves can be found in altimetric data [e.g., *Chelton and Schlax*, 1996; *Killworth et al.*, 1997] and that such waves also exist at mid-latitudes in the southern Indian Ocean. About 4–5 westward propagating events per year were noted in this region [*Schouten et al.*, 2002], and it was shown by *Birol and Morrow* [2001, 2003] that the signals at these latitudes represent approximately semi-annual free Rossby waves originating from the boundary region off West Australia.

[6] When inspecting the current structure at subtropical latitudes, we noted a well-defined zonal band of high mesoscale variability in the latitude range between about

[1]Leibniz-Institute for Marine Sciences (IFM-GEOMAR), Kiel University, Kiel, Germany.
[2]Department of Oceanography, University of Cape Town, Rondebosch, South Africa.

0094-8276/06/2006GL027399

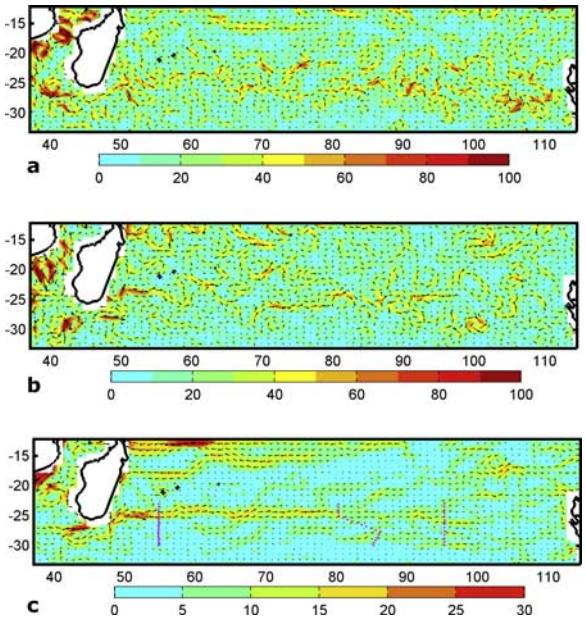

Figure 1. (a) Geostrophic currents on 1 November 2002, (b) on 31 March 2003, and (c) averaged over five years from August 2001 to May 2006. The magenta dots in Figure 1c indicate the positions of the WOCE stations used for transport calculations.

22°S and 26°S. Two examples of geostrophic surface currents are presented in Figures 1a and 1b. One recognizes wave-like and eddy patterns. The signal properties correspond to those of westward-propagating planetary waves which have been well documented in longitude-time plots [e.g., *Birol and Morrow*, 2001, Plate 2]. With the high resolution of the absolute geostrophic current field, one is now able to identify the current structure within the wave trains. The result is a predominantly eastward narrow geostrophic surface current which is guided within the westward propagating Rossby wave structure. The typical widths of the eastward flow in the short-time means are between about 50 and 100 km, mostly within the 22–26°S latitude belt and with speeds reaching beyond 0.5 m/s. However, depending on the phase of the planetary waves, weaker westward flow can also be observed.

[7] The mean over the total period of five years is presented in Figure 1c. In much of the latitude belt 22–26°S, the mean velocities are above 10 cm/s and therefore significant within the error limits of the data set. A continuous mean zonal countercurrent to the east is identified, with a width of about 100–200 km. It is particularly strong between the region off Madagascar and about 80°E where the signal weakens and spreads, becoming well-established again between about 90°E and 100°E. When checking the sequence of events in the data set (see material Animations S1 and S2[1]), a related pattern emerges. Particularly strong eddy and wave formation is recognized in a broad latitude range off West Australia, the suggested region of planetary wave generation [*Birol and Morrow*, 2003]. One finds waves and occasional eddies emanating from this region. The eddies with diameters of 200–300 km appear to be generated off southwestern Australia, travel westward and approach the eastward current belt from the south between 90°S and 80°S. Having grown to wave scale, they become part of the wave structure. This process may be the reason for the lack of a narrow zonal current in this longitude range.

4. Volume Transports

[8] We used the high-resolution meridional WOCE (World Ocean Circulation Experiment) hydrographic sections from 1995 (see Figure 1c) to study the deeper geostrophic current and volume transport structure in the SICC region. The details about how the geostrophic velocity sections were referenced are contained in the auxiliary material. In each section of Figure 2 eastward flow is recognized at latitudes between 23.5°–26°S. When comparing the positions of these cores with geostrophic surface current patterns estimated from Aviso sea level anomalies (DT-MSLA Merged) within a few days of the WOCE observations (not shown), we found excellent correspondence. Although the main flow exists between the surface and 200 dbar as determined in earlier studies, the eastward currents found here in part reach down to 800 dbar or deeper. At 54°E we find two eastward flow cores between 23.5°S and 26°S, with westward flow in between, representing the eastward countercurrent and an anticyclonic eddy south of it. Only a weaker eastward flow core can be identified at 80°E which is the longitude where the eastward flow in Figure 1c weakens and spreads. At 95°E there is a well-defined core again. The 0–800 dbar transports (Figure 3) in the eastward flow cores near 24°S are 10 Sv (54°E), 4 Sv (80°E) and 9 Sv (95°E) with an error estimate of ±3 Sv (1 Sv = 10^6 m^3 s^{-1}). Because of the

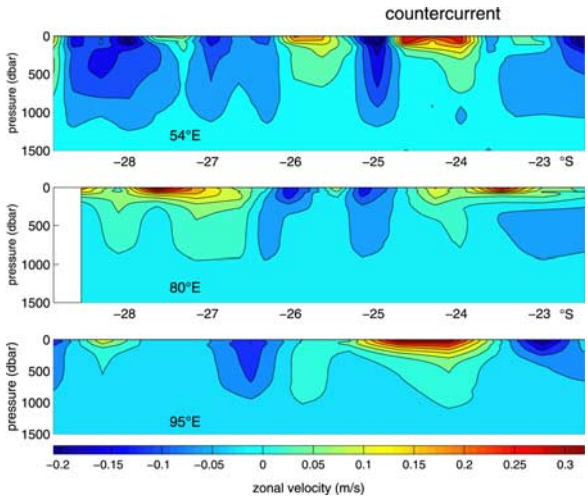

Figure 2. Geostrophic zonal currents (positive to east) at three meridional WOCE sections with the subtropical countercurrent apparent at latitudes around 24°–25°S. The station positions are given in Figure 1c.

[1]Auxiliary materials are available in the HTML. doi:10.1029/2006GL027399.

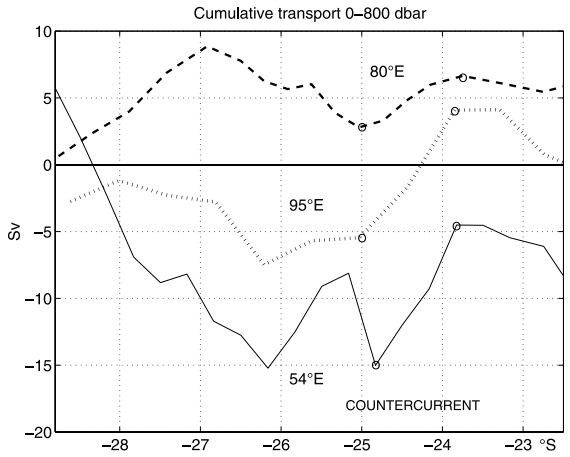

Figure 3. Cumulative geostrophic volume transports (1 Sv = 10^6 m^3 s^{-1}) at three meridional WOCE sections. The station positions are given in Figure 1c. Transports are summed up starting with the southernmost transport station pair. The range between circles indicates the eastward transport in the countercurrent.

smoothing effect due to station distances of about 50 km, the velocities from hydrographic data are somewhat lower than those from the satellite data. The overall transport estimates are not sensitive to station spacing. Since the sections suggest some eastward flow even below 800 dbar, the transport numbers may be on the low side. In a study of transports in the whole water column at 54°E, *Donohue and Toole* [2003] analyzed the same data and also displayed a deep-reaching current band between about 24–25°S with transports of similar size in the upper ocean.

[9] What causes the meridional density gradients which are a prerequisite for the front with a geostrophic countercurrent? The wind stress fields of the southeasterly trades in the north and the westerlies in the south push light water southwestward and heavier water northward. The transition in zonal wind direction occurs near 30°S [see *Kallberg et al.*, 2005] thus generating a subtropical convergence. Surface buoyancy fluxes due to large evaporation minus precipitation in combination with heat flux produces dense water in the eastern South Indian Ocean [e.g., *Schott et al.*, 2002]. The region of maximum surface salinity is found between approximately 25°S and 35°S [*Wyrtki*, 1971; *Toole and Warren*, 1993; *O'Connor et al.*, 2005; *Nauw et al.*, 2006]. The SICC and its related density front coincides with the northern boundary of the maximum surface salinity area and also with the northern boundary of the Subtropical Underwater subduction area [*Karstensen and Quadfasel*, 2002; *O'Connor et al.*, 2005]. We note that one also finds the northern boundary of Subtropical Mode Water formation [*Hanawa and Talley*, 2001] in that region.

[10] Both Ekman transport convergence and surface buoyancy fluxes apparently contribute to generating the SICC related frontal zone. It is not certain at this point which forcing dominates although regional correspondence of salinity pattern and SICC position would seem to suggest a dominating forcing by buoyancy effects in the central and eastern parts of the region. Understanding the processes which control the transition between the western boundary and the central region will require model studies.

5. Origin of the Countercurrent

[11] The results also address the question on the nature of the termination of the southern limb of the East Madagascar Current (EMC). This has variously been described as a complete retroflection [*Lutjeharms*, 1988] based on thermal infrared imagery and drifter tracks, and as a free westward jet generating vortex dipoles [*de Ruijter et al.*, 2004] once it overshoots the southern tip of Madagascar. The lack of an eastward current was a critical argument against the existence of a retroflection [*Quartly et al.*, 2006]. Westward drifting circulation disturbances passing through the region, considered to be eddies, complicate this picture [*Gründlingh et al.*, 1991; *Donohue and Toole*, 2003]. The prevalence of eddies is indeed supported by an animation of events in the region (see auxiliary material). However, when averaging of the altimetric signal is carried out over periods much longer than typical eddy scales, a flow pattern emerges with water from a retroflection of the southern branch of the EMC connected to the subtropical countercurrent. Another part is seen to move directly westward (see Figure 1c).

[12] The EMC has its origin in a branch of the SEC, arriving at the northeastern slope of Madagascar [*Schott et al.*, 1988]. The long-term mean in Figure 1c shows that branch separation already occurs near 60°E and 18°S above the Mascarene Ridge and that a narrow flow band reaches the Madagascar slope and turns south. The mooring data at 23°S by *Schott et al.* [1988] documented southward transports of about 13 and 20 Sv between the surface and 750 m along the Madagascar slope to the south. We also note that the southward transport near Madagascar at 20°S and also the eastward transport near 24–25°S given by *Donohue and Toole* [2003, Figure 20] have magnitudes of more than 10 Sv. The altimeter data are not accurate enough near the coastline (the white area in Figure 1c) to describe the EMC itself. Earlier work, however, has shown it to be a narrow current near the Madagascar slope in that area, with a typical width of 100–200 km [*Schott et al.*, 1988; *Donohue and Toole*, 2003]. Its turning towards the west in the south of Madagascar was not documented by observations directly. However, when inspecting currents below the Ekman layer (148 m) in output from the Simple Ocean Data Assimilation (SODA) package version 1.4.2 [*Carton et al.*, 2000] (J. A. Carton and B. S. Giese, SODA: A reanalysis of ocean climate, submitted to *Journal of Geophysical Research*, 2006, http://iridl.ldeo.columbia.edu/SOURCES/.CARTON-GIESE/SODA/), the EMC can well be followed southward along the east coast and around the southern tip of Madagascar to the west. The model is based on the Geophysical Fluid Dynamics Laboratory MOM 2.b code and assimilates in situ and satellite altimeter data. In all probability the westward flow south of Madagascar seen in Figure 1c therefore represents the continuation of the EMC which partially retroflects and leads into the SICC. The above transport magnitudes mean that the EMC transports would be sufficiently large to provide the source water for the countercurrent. We checked WOCE temperature/salinity diagrams in the core regions of the SEC branch, the EMC and the western SICC (not shown). The curves are variable

in the SEC, and the envelopes of distributions correspond and are tight in the EMC and SICC between 150 and 800 dbar, supporting the conclusion that the flows are related.

[13] *Palastanga et al.* [2006] described an anticyclonic cell between Madagascar and about 75°E, bounded by the SEC in the north and the SICC in the south. In Figure 1c there is only a hint of a northward flow between 70° and 75° closing such a cell in the east.

6. Conclusions

[14] With its rather large transport of O(10 Sv) the SICC is an essential component of the near-surface subtropical circulation in the South Indian Ocean. The core of the zonal countercurrent extends to about 800 m. This is similar to the subtropical countercurrent in the North Atlantic where persistent eastward flow was observed at 700 m [*Rossby et al.*, 1983] and the transport was estimated at about 10 Sv [*Schmitz*, 1996]. In the Pacific, however, the current cores were found at shallower depths, above about 250 m [*Qiu*, 1999; *Qiu and Chen*, 2004].

[15] The present study shows evidence for a narrow SICC being embedded in a planetary wave and eddy flow pattern. The source region for a considerable part of the variability was earlier found in the southwest of Australia. In addition, baroclinic instability can be expected to play a role in the more central parts of the subtropical South Indian Ocean. Potential vorticity distributions at approximately 250 m and 500 m [*McCarthy and Talley*, 1999] show a change of sign in the region to the north, between the SICC and the SEC, corresponding to the necessary condition for baroclinic instability [e.g., *Kantha and Clayson*, 2000].

[16] Based on a 5-year mean we show that the EMC is fed by a well-defined branch of the SEC. At the southern termination of the EMC there is evidence for both the EMC retroflecting and thus feeding the SICC and for moving directly westward. The energetic eddy pattern makes it difficult to recognize a possible dominance of westward jet or eastward retroflection during shorter periods. The countercurrent advects water to the subtropical underwater subduction region, probably influencing the composition of water masses in the subduction process. The dynamics of the frontal zone and the corresponding countercurrent generation remain to be clarified although it can be imagined that surface buoyancy fluxes dominate the wind stress influence.

[17] Zonal jets like the SICC appear to be common features of the subtropical circulation. The global maps of *Maximenko et al.* [2005] obtained from Aviso 10-year anomalies indicate subtropical bands with predominantly eastward, but also with some westward current components in the North and South Pacific and the South Indian Ocean, and somewhat further poleward at 35°S in the South Atlantic Ocean. Zonal flow bands may well be a more important feature of the general subtropical circulation than was usually assumed.

[18] **Acknowledgments.** The study was supported by the National Research Foundation and the Water Research Commission of South Africa as well as the University of Cape Town. G. S. expresses his gratitude for the Alexander von Humboldt Award that made this study possible. The altimeter products were produced by Ssalto/Duacs and distributed by Aviso, with support from CNES. The data set Rio05 was produced by the CLS Space Oceanography Division.

References

Aoki, S., and S. Imawaki (1996), Eddy activities of the surface layer in the western North Pacific detected by satellite altimeter and radiometer, *J. Oceanogr.*, *52*, 457–474.

Birol, F., and R. Morrow (2001), Source of the baroclinic waves in the southeast Indian Ocean, *J. Geophys. Res.*, *106*(C9), 145–160.

Birol, F., and R. Morrow (2003), Separation of quasi-semiannual Rossby waves from the eastern boundary of the Indian Ocean, *J. Mar. Res.*, *61*, 707–723.

Carton, J. A., G. A. Chepurin, X. Cao, and B. Giese (2000), A Simple Ocean Data Assimilation retrospective analysis of the global ocean 1950–1995: Part I. Methodology, *J. Phys. Oceanogr.*, *30*, 294–309.

Chelton, D. B., and M. G. Schlax (1996), Global observations of oceanic Rossby waves, *Science*, *272*, 234–238.

de Ruijter, P. M., H. M. van Aken, E. J. Beier, J. R. E. Lutjeharms, R. P. Matano, and M. W. Schouten (2004), Eddies and dipoles around South Madagascar: Formation, pathways and large-scale impact, *Deep Sea Res., Part I*, *51*, 383–400.

Donohue, K. A., and J. M. Toole (2003), A near-synoptic survey of the Southwest Indian Ocean, *Deep Sea Res., Part II*, *50*, 1893–1931.

Gründlingh, M. L., R. A. Carter, and R. C. Stanton (1991), Circulation and water properties of the southwest Indian Ocean, spring 1987, *Prog. Oceanogr.*, *28*(4), 305–342.

Hanawa, K., and L. D. Talley (2001), Mode waters, in *Ocean Circulation and Climate*, edited by G. Siedler, J. Church, and J. Gould, pp. 373–386, Elsevier, New York.

Hansen, D. V., and P. M. Poulain (1996), Quality control and interpolation of WOCE/TOGA drifter data, *J. Atmos. Oceanic Technol.*, *13*, 900–909.

Kallberg, P., P. Berrisford, B. Hoskins, A. Simmmons, S. Uppala, S. Lamy-Thépaut, and R. Hine (2005), *ERA-40 Atlas*, 191 pp., Eur. Cent. for Medium-Range Weather Forecasts, Reading, U. K.

Kantha, L. H., and C. A. Clayson (2000), *Numerical Models of Oceans and Oceanic Processes*, 940 pp., Elsevier, New York.

Karstensen, J., and D. Quadfasel (2002), Water subducted into the Indian Ocean subtropical gyre, *Deep Sea Res., Part II*, *49*, 1441–1457.

Killworth, P. D., D. B. Chelton, and R. A. de Szoeke (1997), The speed of observed and theoretical long extra-tropical planetary waves, *J. Phys. Oceanogr.*, *27*, 1946–1966.

Levitus, S., J. I. Antonov, T. P. Boyer, and C. Stephens (2001), *World Ocean Database 1998* [CD-ROM], *WOD98*, Natl. Oceanic and Atmos. Admin., Silver Spring, Md.

Lutjeharms, J. R. E. (1988), Remote sensing corroboration of retroflection of the East Madagascar Current, *Deep Sea Res.*, *35*, 2045–2050.

Maximenko, N. A., B. Bang, and H. Sasaki (2005), Observational evidence of alternating zonal jets in the world ocean, *Geophys. Res. Lett.*, *32*, L12607, doi:10.1029/2005GL022728.

McCarthy, M. C., and L. D. Talley (1999), Three-dimensional isoneutral potential vorticity structure in the Indian Ocean, *J. Geophys. Res.*, *104*(C6), 13,251–13,267.

Merle, J., H. Rotschi, and B. Voituriez (1969), Zonal circulation in the tropical western South Pacific at 170°E, in *Professor Uda's Commemorative Papers*, *Bull. Jpn. Soc. Fish. Oceanogr.*, special issue, 91–98.

Nauw, J. J., H. M. van Aken, J. R. E. Lutjeharms, and W. P. M. de Ruijter (2006), Intrathermocline eddies in the Southern Indian Ocean, *J. Geophys. Res.*, *111*, C03006, doi:10.1029/2005JC002917.

Niiler, P. P., A. Sybrandy, K. Bi, P. Poulain, and D. Bitterman (1995), Measurements of the water-following capability of Holey-sock and TRISTAR drifters, *Deep Sea Res., Part I*, *42*, 1951–1964.

O'Connor, B. M., R. A. Fine, and D. B. Olson (2005), A global comparison of subtropical underwater formation rates, *Deep Sea Res., Part I*, *52*, 1569–1590.

Palastanga, V., P. J. van Leeuwen, M. W. Schouten, and W. P. M. de Ruijter (2006), Flow structure and variability in the subtropical Indian Ocean: Instability of the South Indian Ocean Countercurrent, *J. Geophys. Res.*, doi:10.1029/2005JC003395, in press.

Qiu, B. (1999), Seasonal eddy field modulation of the North Pacific Subtropical Countercurrent: TOPEX/Poseidon observations and theory, *J. Phys. Oceanogr.*, *29*, 2471–2486.

Qiu, B., and S. Chen (2004), Seasonal modulations in the eddy field of the South Pacific Ocean, *J. Phys. Oceanogr.*, *34*, 1515–1527.

Quartly, G. D., J. J. H. Buck, M. A. Srokosz, and A. C. Coward (2006), Eddies around Madagascar—The retroflection re-considered, *J. Mar. Syst.*, *63*, 115–129, doi:10.1016/j.jmarsys.2006.06.001.

Reid, J. L. (2003), On the total geostrophic circulation of the Indian Ocean: Flow patterns, tracers and transports, *Prog. Oceanogr.*, *56*, 137–186.

Rio, M.-H., and F. Hernandez (2004), A mean dynamic topography computed over the world ocean from altimetry, in situ measurements,

and a geoid model, *J. Geophys. Res.*, *109*, C12032, doi:10.1029/2003JC002226.

Rossby, H. T., S. C. Riser, and A. J. Mariano (1983), The western North Atlantic—A Lagrangian viewpoint, in *Eddies in Marine Science*, edited by A. R. Robinson, pp. 66–91, Springer, New York.

Schmitz, W. J. (1996), *On the World Ocean Circulation*, vol. 1, *WHOI Tech. Rep. WHOI-96-03*, 141 pp., Woods Hole Oceanogr. Inst., Woods Hole, Mass.

Schott, F., M. Fieux, J. Kindle, J. Swallow, and R. Zantopp (1988), The boundary currents east and north of Madagascar: 2. Direct measurements and model comparison, *J. Geophys. Res.*, *93*(C5), 4963–4974.

Schott, F. A., M. Dengler, and R. Schoenefeldt (2002), The shallow overturning circulation of the Indian Ocean, *Progr. Oceanogr.*, *53*, 57–103.

Schouten, M. W., W. P. M. de Ruijter, and P. J. van Leeuwen (2002), Upstream control of the Agulhas ring shedding, *J. Geophys. Res.*, *107*(C8), 3110, doi:10.1029/2001JC000864.

Stramma, L., and J. R. E. Lutjeharms (1997), The flow field of the subtropical gyre in the South Indian Ocean, *J. Geophys. Res.*, *102*(C3), 5513–5530.

Toole, J. M., and B. A. Warren (1993), A hydrographic section across the subtropical South Indian Ocean, *Deep Sea Res., Part I*, *40*, 1973–2019.

Wyrtki, K. (1971), *Oceanographic Atlas of the International Indian Ocean Expedition*, *OCE/NSF 86-00-001*, 531 pp., Nat.l Sci. Found., Washington, D. C.

Wyrtki, K. (1975), Fluctuations of the dynamic topography in the Pacific Ocean, *J. Phys. Oceanogr.*, *5*, 450–459.

J. R. E. Lutjeharms and M. Rouault, Department of Oceanography, University of Cape Town, 7700 Rondebosch, South Africa.

G. Siedler, Leibniz-Institute for Marine Sciences (IFM-GEOMAR), Kiel University, D-24105 Kiel, Germany. (gsiedler@ifm-geomar.de)